Targeting dual oncogenic machineries driven by TAL1 and PI3K-AKT pathways in T-cell acute lymphoblastic leukemia

Fang Qi Lim,[1] Allison Si-Yu Chan,[1] Rui Yokomori,[1] Xiao Zi Huang,[1] Madelaine Skolastika Theardy,[1] Allen Eng Juh Yeoh,[1,2] Shi Hao Tan[1] and Takaomi Sanda[1,3]

[1]Cancer Science Institute of Singapore, National University of Singapore; [2]VIVA-NUS CenTRAL, Department of Pediatrics, National University of Singapore and [3]Department of Medicine, Yong Loo Lin School of Medicine, National University of Singapore, Singapore

Correspondence: T. Sanda
takaomi_sanda@nus.edu.sg

Received: January 27, 2022.
Accepted: August 30, 2022.
Prepublished: September 8, 2022.

https://doi.org/10.3324/haematol.2022.280761

Abstract

T-cell acute lymphoblastic leukemia (T-ALL) is a malignancy of thymic T-cell precursors. Overexpression of oncogenic transcription factor *TAL1* is observed in 40-60% of human T-ALL cases, frequently together with activation of the NOTCH1 and PI3K-AKT pathways. In this study, we performed chemical screening to identify small molecules that can inhibit the enhancer activity driven by TAL1 using the *GIMAP* enhancer reporter system. Among approximately 3,000 compounds, PIK-75, a known inhibitor of PI3K and CDK, was found to strongly inhibit the enhancer activity. Mechanistic analysis demonstrated that PIK-75 blocks transcriptional activity, which primarily affects TAL1 target genes as well as AKT activity. TAL1-positive, AKT-activated T-ALL cells were very sensitive to PIK-75, as evidenced by growth inhibition and apoptosis induction, while T-ALL cells that exhibited activation of the JAK-STAT pathway were insensitive to this drug. Together, our study demonstrates a strategy targeting two types of core machineries mediated by oncogenic transcription factors and signaling pathways in T-ALL.

Introduction

T-cell acute lymphoblastic leukemia (T-ALL) is a malignant disorder resulting from the leukemic transformation of T-cell precursors.[1-5] This disease is characterized by aberrant expression of oncogenic transcription factors such as *TAL1*, *TAL2*, *TLX1*, *TLX3*, *LMO1*, *LMO2*, *HOXA* and *NKX2-1*, which are exclusively expressed and define distinct molecular subgroups[1-5] (called "type A" abnormalities).[4] Although recent developments in small-molecule inhibitors have produced remarkable clinical results against certain malignancies, such benefits have not been obtained in T-ALL. Therefore, further advances in prognosis require improved knowledge of T-ALL pathogenesis and the identification of novel therapeutic drugs for this disease.

TAL1 is one of the most prevalent oncogenes in T-ALL and is aberrantly overexpressed in 40-60% of human T-ALL cases.[6-8] We previously reported that TAL1 forms an interconnected autoregulatory loop with its regulatory partners (GATA3 and RUNX1) in T-ALL cells,[9] which likely contributes substantially to sustaining the oncogenic transcriptional program. We also identified several critical downstream targets and their enhancers, including the *GIMAP* and *ARID5B* genes,[10-13] that are directly activated by TAL1 under the control of super-enhancers in T-ALL cells. Interestingly, multiple *GIMAP* genes, which are located within a gene cluster, are regulated by a single enhancer element in T-ALL cells. TAL1, GATA3, and RUNX1 activate this enhancer, while the tumor suppressor E-proteins (E2A and HEB) inhibit this activity. This element is also directly regulated by NOTCH1,[13] another prevalent oncogene in T-ALL.[14] Thus, the activity of the *GIMAP* enhancer represents the status of oncogenic transcription factors and tumor suppressors in T-ALL cells.

Besides type A abnormalities, many studies have demonstrated that several molecular abnormalities, many of which are pro-proliferative and pro-survival signaling pathways, are shared across different T-ALL subgroups[1-5] (called "type B" abnormalities).[4] They are often simultaneously present and cooperate with type A abnormalities in T-ALL. These abnormalities include genetic mutations

in PI3K-AKT-PTEN pathway components, which are more frequently observed in *TAL1*-positive T-ALL (approximately 50%) than in other subgroups (7-30%), while activation of the JAK-STAT pathway is more frequently observed in *TLX1/3*-positive T-ALL (43%).[15,16] These genetic relationships suggest preferential combination and cooperative effects between specific type A and type B abnormalities. In other words, it is ideal to concurrently block such cooperative mechanisms as a therapeutic strategy.

In this study, we began with chemical screening to identify small molecules that can inhibit enhancer activity driven by the TAL1 complex using the *GIMAP* enhancer reporter system. This pinpointed PIK-75, a known inhibitor of PI3K and cyclin-dependent kinases (CDK), which exerts potent cytotoxicity through inhibition of TAL1 and PI3K-AKT pathways. Our study proposes a strategy targeting dual oncogenic mechanisms driven by type A and B abnormalities in T-ALL cells.

Methods

Cell culture and reagents

All T-ALL cell lines and 293T cells were cultured in RPMI-1640 and DMEM medium (BioWest), respectively, supplemented with 10% fetal bovine serum (BioWest) in a CO_2 incubator. For interleukin-7 (IL-7) stimulation, HPB-ALL and SUP-T1 cells were cultured with 50 ng/mL recombinant human IL-7 (PeproTech) for 24 hours. Dibenzazepine (DBZ) was purchased from Tocris. THZ1 and (+)-JQ1 were purchased from Selleck Chemicals. WP1130 and PIK-75 were purchased from MedChemExpress.

Patient-derived xenograft model

Two human T-ALL patient-derived xenograft (PDX) samples (DFCI-9 and DFCI-15) were kindly provided by Dr Alejandro Gutierrez and were expanded in NOD-SCID-γ mice via tail vein injection. Human leukemic cells were harvested from moribund mice and sorted by fluorescence-activated cell sorting (FACS) using an anti-human CD45-APC antibody (BioLegend) by BD FACS ARIA. The protocol was approved by the Institutional Animal Care and Use Committee of the National University of Singapore.

Chemical screening

Chemical screening was performed at the Center for High-throughput Phenomics, Genome Institute of Singapore (CHiP-GIS). Briefly, Jurkat cells stably transduced with the *eGIMAP-luciferase* construct were seeded in 384-well plates at 2,500 cells per well. After 24 hours, compounds from the Epigenetics 151 Library (151 compounds, 2 μM, duplicates), Anticancer Library (414 compounds, 1 μM, triplicates), and Spectrum Collection (2,396 compounds, 1 μM, triplicates), dimethyl sulfoxide (DMSO), and THZ1 (1 μM) were added using a liquid handling workstation. Five hours after incubation, cell viability (fluorescence) and enhancer activity (luminescence) were measured using the ONE-Glo+Tox Luciferase Reporter and Cell Viability Assay (Promega) using a microplate reader (Tecan). The readout was normalized among the replicates.

Knockdown and overexpression experiments

Short hairpin RNA (shRNA) sequences are listed in the *Online Supplementary Table S1*. Each sequence was cloned into pLKO.1-puro lentiviral vector. 293T cells were transfected with envelope plasmid pMD2.G, packaging plasmids pMDLg/pRRE and pRSV-Rev, and the corresponding shRNA constructs using FuGENE 6 transfection reagent (Promega) and Opti-MEM (Gibco). Jurkat cells were spinoculated with filtered virus-containing medium supplemented with polybrene (Sigma-Aldrich). Puromycin was added 36 hours post infection. For BCL2 overexpression, 293T cells were transfected with pMSCV-GFP-BCL2,[11] packaging plasmid gag-pol, and envelope plasmid VSV-G using FuGENE 6 transfection reagent and Opti-MEM. Jurkat cells were spinoculated with filtered virus-containing medium supplemented with polybrene.

RNA extraction and quantitative reverse transcription polymerase chain reaction

Total RNA was extracted using a NucleoSpin RNA kit (Macherey-Nagel). A total of 1,000 ng RNA and 1 μL of ERCC Spike-In (1:100 dilution) (Invitrogen) was reverse-transcribed into cDNA using iScript cDNA Synthesis Kit (Bio-Rad). Quantitative polymerase chain reaction (qPCR) was performed using Power SYBR Green PCR Master Mix (Applied Biosystems) on the Quant Studio 3 System (Thermo Fisher Scientific). mRNA expression levels were evaluated using the ΔΔ Ct method. Primer sequences are listed in the *Online Supplementary Table S2*.

Protein extraction and western blot analysis

Cells were lysed with Cell Lysis Buffer (Cell Signaling Technology) supplemented with protease inhibitor (Thermo Scientific). Proteins were separated by SDS-PAGE and transferred onto polyvinylidene difluoride membranes (Bio-Rad). The antibodies used are listed in the *Online Supplementary Table S3*.

Cell viability assay

Cell lines were seeded at 5,000 cells per well into 96-well plates. Cell viability was measured after treatment with inhibitors by measuring the luminescence using a CellTiter-Glo assay (Promega). The half maximal inhibitory concentration (IC_{50}) values were determined by the dose response inhibition function using variable slope by GraphPad Prism.

Flow cytometric analysis

For the apoptosis assay, cells were treated with PIK-75 at the corresponding IC_{80} values for 4 hours and were stained with AnnexinV-APC (BioLegend) and propidium iodide (Sigma) for 15 minutes. The cells were then analyzed by flow cytometry (BD, LSR II) and FlowJo.

RNA sequencing analysis

Sample preparation

ERCC RNA spike-in controls (1:10) were added at 1 uL per 1 million cells. Total RNA was extracted using QIAzol reagent, miRNeasy Mini Kit, and DNase I (Qiagen). Strand-specific library construction and 100-bp paired-end sequencing with a sequencing depth of 20 M reads on DNBseq were performed at BGI Genomics.

Data processing

RNA sequencing (RNA-seq) reads were mapped to transcript sequences of curated RefSeq and ERCC spike-in controls using salmon (version 1.1.0)[17] with the options "--gcBias --seqBias –validateMappings". The index file for the transcript sequences was created with default settings. Transcript-level read counts were converted to gene-level read counts using tximport (version 1.14.2).[18] The genes that did not have more than five read counts in at least two samples were removed. The gene level read counts were normalized using upper quantile normalization, and those of spike-in controls were used to estimate the factor (k=1) of unwanted variation between samples using RUVSeq (version 1.20.0).[19] Differentially expressed genes were then estimated using DESeq2 (version 1.26.0).[20,21] The estimated unwanted factor was included in the design formula of DESeq2 for spike-in normalization.

Gene set enrichment analysis and gene ontology analysis

Gene set enrichment analysis (GSEA)[22] analysis was performed on the normalized RNA-seq data. High-confidence targets of TAL1 were previously defined[12] by identifying genes that have enhancer regions bound by TAL1 and are also downregulated by the knockdown. Super-enhancer-associated genes were also previously defined,[12] which possess super-enhancers in Jurkat but not in normal thymus, Th1, Th2 or Th17 cells. Gene ontology (GO) analysis was performed using the Enrichr tool.[23] The top 10 categories with the lowest adjusted *P* value were selected.

Statistical analysis

Statistical analysis was performed for the results which were done with biological replicates. Comparisons were performed with Student's *t*-tests, and *P* values denoted as **P*<0.05, ***P*<0.01, or ****P*<0.001 were deemed significant (NS, not significant). Standard deviation (SD) was not shown for the results which were done in duplicates.

Dataset availability

RNA-seq data has been deposited in the Gene Expression Omnibus database under accession numbers GSE181435.

Results

Establishment of the *GIMAP* enhancer reporter system

In our previous study, we identified an enhancer element regulating multiple *GIMAP* genes within the *GIMAP* gene cluster[13] (also shown in the *Online Supplementary Figure S1A*). This element was bound by TAL1, its regulatory partners (GATA3 and RUNX1) and coactivators (e.g., CBP) in a T-ALL cell line (Jurkat). The same position was also bound by NOTCH1. Notably, this element was associated with a super-enhancer in multiple T-ALL cell samples, thus showing that it is highly activated in T-ALL cells. We cloned the enhancer sequence into a luciferase reporter construct, which was shown to be activated by TAL1 and its regulatory partners and inhibited by E-proteins in T-ALL cells.

In the current study, we utilized this reporter system as a readout to evaluate the overall transcriptional activity. Using this system, we aimed to identify drugs that can globally inhibit transcriptional activity mediated by TAL1 rather than focusing on specific function or expression of *GIMAP* genes. We established a Jurkat subclone that stably expressed the reporter construct (Figure 1A). Under this condition, *luciferase* expression can be induced by transcription factors endogenously expressed in Jurkat cells. As a proof of principle, we confirmed that genetic knockdown of *TAL1* or its regulatory partners by shRNA significantly inhibited *luciferase* activity (Figure 1B). Pharmacological inhibition of NOTCH1 activity with DBZ, a γ-secretase inhibitor (GSI), moderately inhibited *luciferase* activity (Figure 1C) compared to vehicle (DMSO) (*Online Supplementary Figure S1B*), suggesting that the *GIMAP* enhancer is not completely dependent on NOTCH1 activity. We also confirmed that a small-molecule inhibitor of CDK7 (THZ1) that inhibits the activation of RNA polymerase II[24] strongly downregulated *luciferase* activity after 5 hours of treatment (Figure 1C). Thus, THZ1 serves as a positive control.

Of note, T-ALL cells, including Jurkat cells, are known to be sensitive to transcription inhibition by THZ1 treatment.[24] Cell viability was significantly inhibited after 24 hours of treatment (*Online Supplementary Figure S1C*). Thus, in order to minimize indirect or non-specific effects on transcription due to growth inhibition, we decided to measure luciferase activity only after 5 hours of drug treatment.

Small-molecule screening identified PIK-75, which inhibits *GIMAP* enhancer activity

We then performed a chemical screening using this reporter system to identify small molecules that can block the enhancer activity driven by oncogenic transcription

factors. We applied three small-molecule libraries ("spectrum collection", "epigenetic library", and "anticancer library"), which included a total of approximately 3,000 commercially-available compounds (Figure 2A). We measured both enhancer activity and cell viability in technical duplicates 5 hours after drug addition. The results were compared to DMSO (negative control) and THZ1 (positive control) (Figure 2B for anticancer library; *Online Supplementary Table S4*).

As expected, THZ1 strongly inhibited enhancer activity

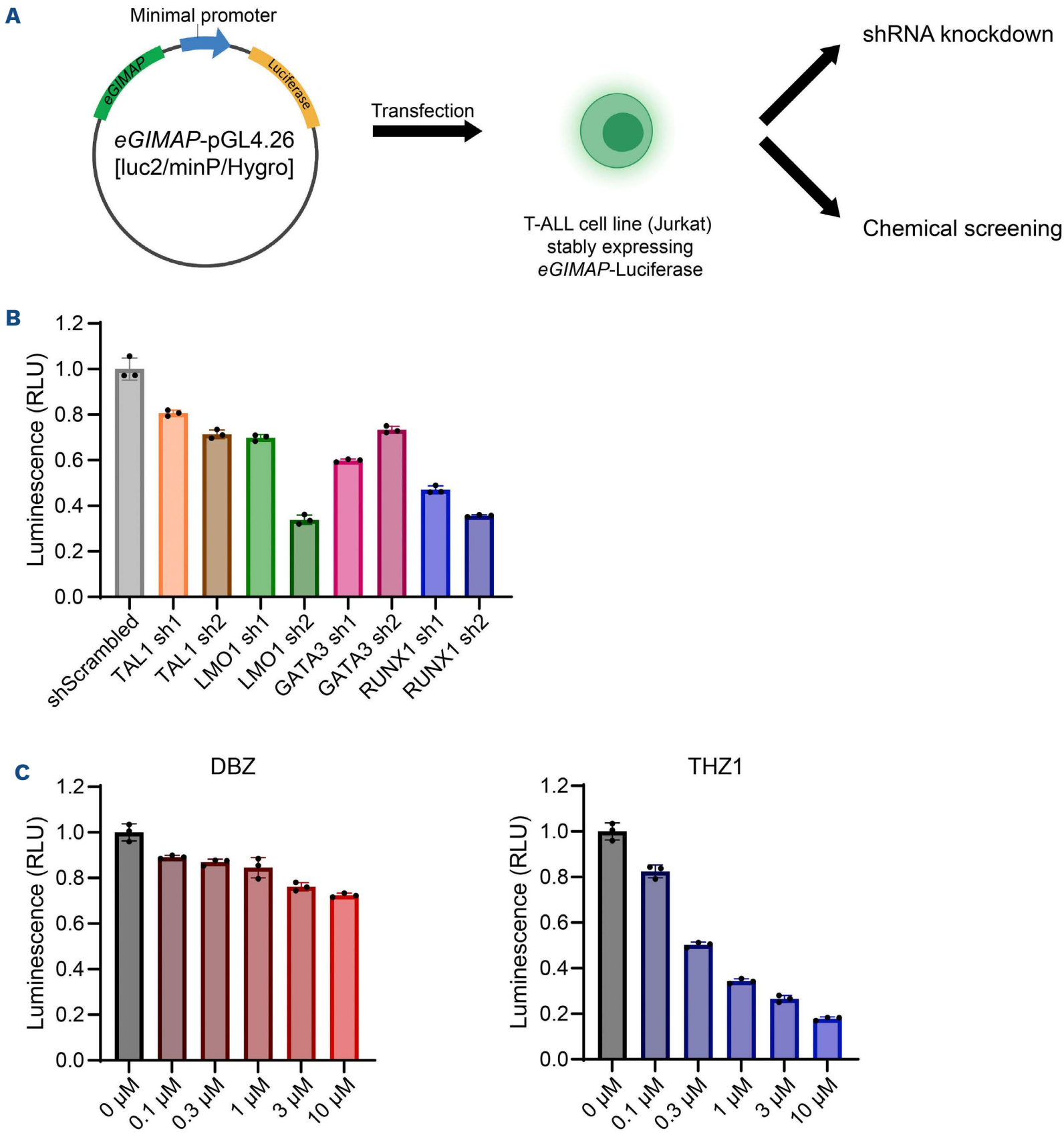

Figure 1. Establishment of the *GIMAP* enhancer reporter system. (A) Overview of the strategy used to screen for small-molecule compounds. The *GIMAP* enhancer luciferase reporter construct (*eGIMAP*-pGL4.26) was cloned and transfected into Jurkat cells. Stable clones were selected and subjected to drug screening or genetic knockdown. (B) Jurkat cells stably expressing the *GIMAP* reporter construct were subjected to short hairpin RNA (shRNA) knockdown using lentivirus infection. Cell viability and *luciferase* activity were measured 3 days post infection. Relative luminescence was determined by normalizing luciferase activity to cell viability and is presented as the fold change compared to the control scrambled RNA (shScrambled RNA). The values are shown as individual dots and the mean ± standard deviation of technical triplicates. (C) Jurkat cells stably expressing the *GIMAP* reporter construct were treated with DBZ or THZ1. Cell viability and *luciferase* activity were measured after 5 hours. Relative luminescence was determined by normalizing *luciferase* activity to cell viability and is presented as the fold change compared to untreated cells (0 nM). The values are shown as individual dots and the mean ± standrard devaition of technical triplicates. Representative results from multiple independent experiments were shown (B and C).

(shown in red) as compared to DMSO (shown in orange) and the majority of compounds. In contrast, several cytotoxic agents (obatoclax mesylate, PHA-665752, CNX-2006, osimertinib, and AZ5104) dominantly reduced cell viability but not enhancer activity (shown in purple), suggesting that the mechanism of growth inhibition of these compounds is independent of transcription activities. We then shortlisted the compounds that showed stronger reduction in enhancer activity than THZ1 (fold change of luminescence compared to THZ1 <0.5). Notably, two compounds (PIK-75 and WP1130) were statistically significant (P<0.05, shown in green). These drugs also reduced cell viability, demonstrating strong cytotoxicity at even short time points. Independent validation showed that treatment with PIK-75 significantly inhibited enhancer activity in a dose-dependent manner (Figure 2C), similar to the results of THZ1 treatment. However, WP1130 inhibited the activity only at high concentrations (over 3 μM) and thus was not selected for the downstream analysis.

Of note, PIK-75 was originally developed as an inhibitor that blocks PI3K p110α activity.[25] Later studies showed that PIK-75 also inhibits other kinases including CDK.[25,26] Hence, this drug has multiple targets besides PI3K. In contrast, 34 other small molecules included in our chemical screening (e.g., PI-103), which have been reported to specifically inhibit PI3K or its downstream AKT or mTOR, did not show a stronger inhibitory effect than PIK-75 on luciferase (0.174 for PIK-75, and 0.502-1.188 for 34 drugs) or

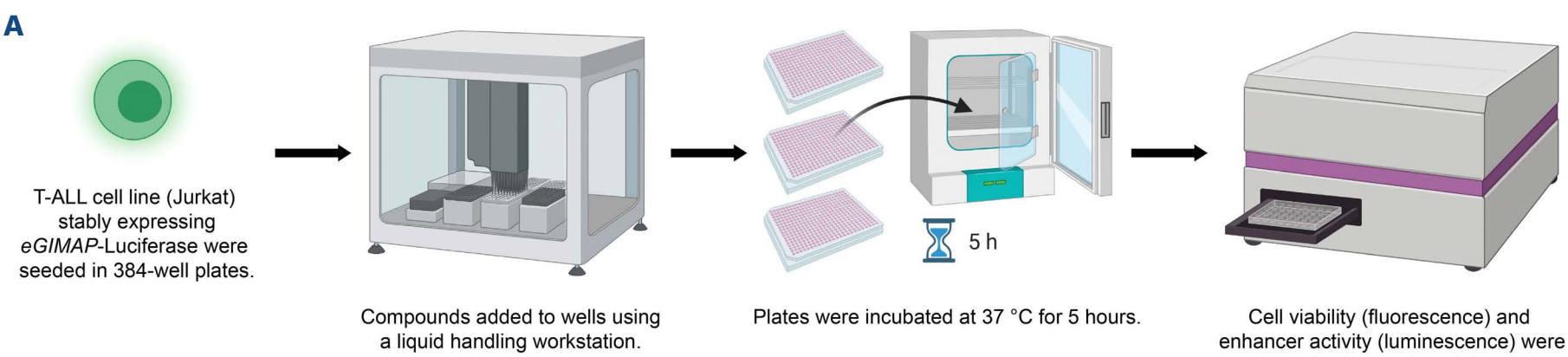

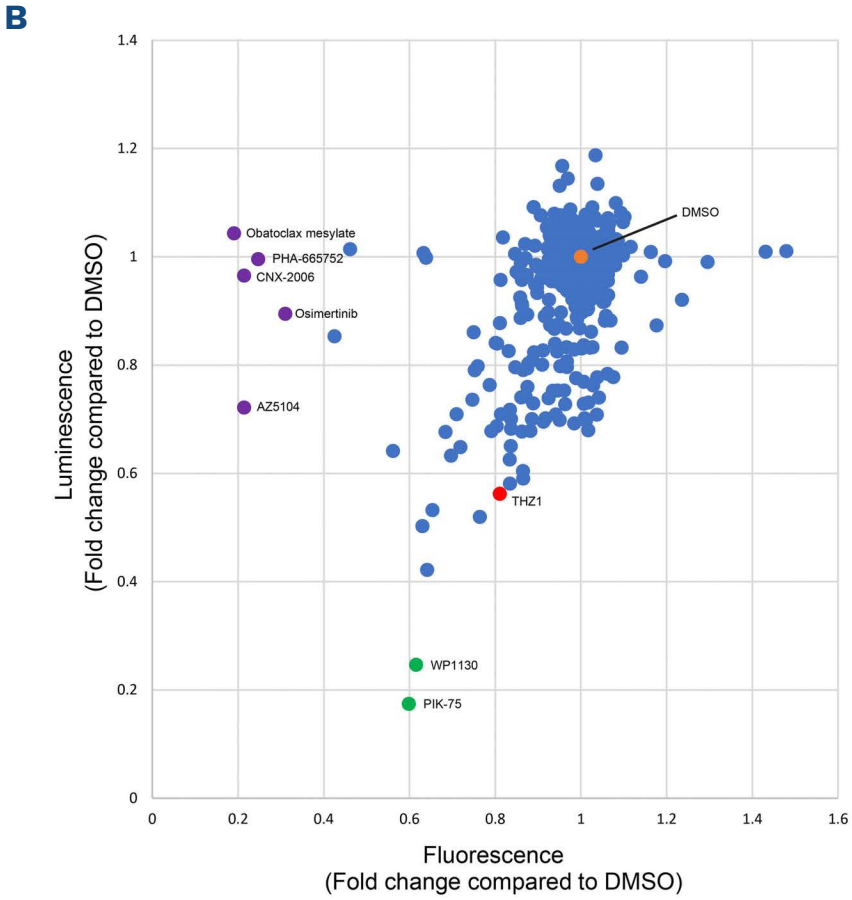

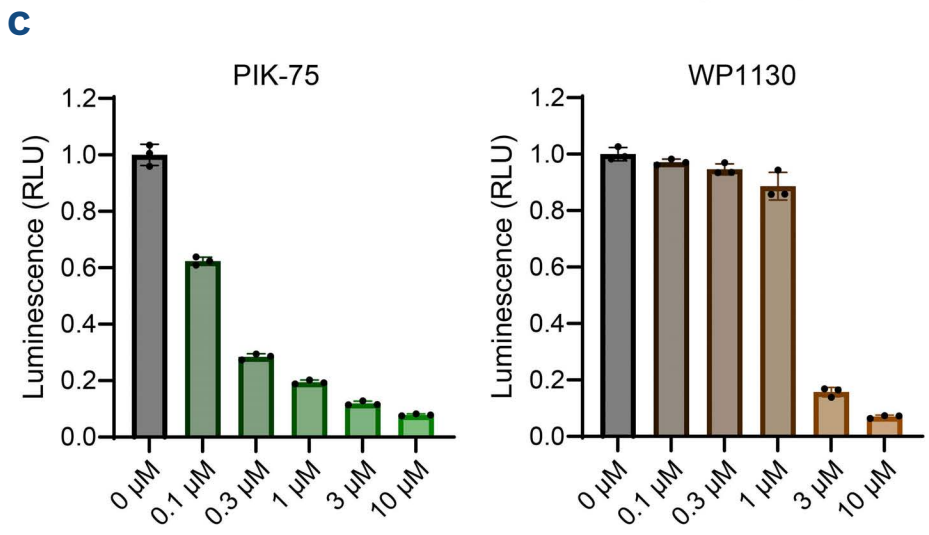

Figure 2. Chemical screening using the *GIMAP* enhancer reporter system. (A) Overview of the chemical screening strategy. Using a liquid handling workstation, 2,961 compounds from 3 chemical libraries, a negative control (dimethyl sulfoxide [DMSO]) and a positive control (THZ1), were added to Jurkat cells that stably expressed the *GIMAP* enhancer reporter construct. Cell viability and *luciferase* activity were measured after 5 hours using a microplate reader. Images were created by BioRender. (B) Scatterplot showing luminescence (representing the *GIMAP* enhancer activity) and fluorescence (representing cell viability) of the cells treated with each of the compounds from the anticancer library. The values shown are the means of technical triplicates, presented as fold change compared to THZ1. (C) Jurkat cells stably expressing the *GIMAP* enhancer construct were treated with PIK-75 and WP1130 at various concentrations. Cell viability and *luciferase* activity were measured after 5 hours. Relative luminescence was determined by normalizing *luciferase* activity to cell viability and is presented as the fold change compared to untreated cells. The values are shown as individual dots and the mean ± standard deviation of technical triplicates. Representative results from multiple independent experiments were shown (C).

cell viability (0.599 for PIK-75, and 0.630-1.076 for 34 drugs) (*Online Supplementary Table S4*). Similarly, A66, which is a more potent inhibitor of p110a subunit of PI3K, did not show a stronger growth inhibitory effect (*Online Supplementary Figure S2*). This suggested that the effect of PIK-75 is not solely attributed to the inhibition of PI3K, which prompted us to investigate detailed molecular mechanisms.

PIK-75 treatment inhibits cell growth and induces apoptosis in T-cell acute lymphoblastic leukemia cells

We first examined the growth inhibitory effect of PIK-75 after 24 hours of treatment across different cell lines, to find if there are any factors associated with the sensitivity. Prior to this, we analyzed the status of AKT, a downstream target of PI3K, which demonstrated that AKT was constitutively phosphorylated on Ser473 in many T-ALL cell lines, most of which were *TAL1*-positive cell lines (Figure 3A). Of note, we could not find any *TAL1*-positive cell line without AKT phosphorylation in our stock, suggesting a potential requirement of AKT activity in those T-ALL cases when established in culture. This is similar to the observation in primary human T-ALL cases in which *TAL1* overexpression was frequently observed with genetic mutations of the PI3K-AKT pathway.[15] Interestingly, we observed a notable difference in drug sensitivity (Figure 3B). Cell lines with viability greater than 20% after treatment with 1 μM PIK-75 at 24 hours, for which IC_{50} values could not be determined (N.D.), were considered to be insensitive. *TAL1*-positive T-ALL cell lines were found to be very sensitive to this inhibitor, for which the IC_{50} values were 59-96 nM (Figure 3C and D). In particular, five TAL1-positive cell lines that exhibited constitutive AKT phosphorylation on Ser473 (MOLT-16, MOLT-4, Jurkat, CCRF-CEM, RPMI-8402) were more sensitive than those that exhibited constitutive AKT phosphorylation but did not express TAL1 (SUP-T1, HPB-ALL, LOUCY, P12-ICHIKAWA) (Figure 3C and D). In contrast, four T-ALL cell lines that did not express TAL1 nor exhibit phosphorylated AKT (KOPT-K1, ALL-SIL, DND-41, TALL-1) were the least sensitive (IC_{50} values N.D.). In particular, DND-41 cells were strongly insensitive to PIK-75 (yellow lines in Figure 3B and C). It is noteworthy that these four lines have been previously reported to be sensitive to GSI.[27] Additionally, ALL-SIL cells that do not express TAL1 but harbor the *NUP214-ABL1* fusion[28] were insensitive to this drug (gray lines in Figure 3B and C). Comparison among three groups of cell lines based on TAL1 and AKT status ("TAL1+pAKT+", "TAL1-pAKT+", and "TAL1-pAKT-") showed that "TAL1+/pAKT+" cell lines (MOLT-16, MOLT-4, Jurkat, CCRF-CEM, RPMI-8402 and PF-382) were most sensitive (IC_{50} values 59-96 nM) with an exception of PF-382 (N.D.). "TAL1-/pAKT+" cell lines (SUP-T1, HPB-ALL, LOUCY and P12-ICHIKAWA) were relatively sensitive (IC_{50} values 105-172 nM) with the exception of LOUCY and P12-ICHIKAWA (N.D.), while "TAL1-pAKT-" cell lines (KOPT-K1, ALL-SIL, DND-41 and TALL-1) were least sensitive (N.D.). These results suggested that drug sensitivity is associated with TAL1 and AKT status.

We next analyzed cellular phenotypes after PIK-75 treatment. We used 120 nM, which is the IC_{80} of a sensitive cell line, Jurkat. This analysis showed that apoptosis was induced in Jurkat as early as at 4 hours (Figure 3E; *Online Supplementary Figure S3A*), which was more evident at higher doses at 24 hours (*Online Supplementary Figure S3B*). In contrast, there was not much increase in an insensitive cell line (DND-41) (*Online Supplementary Figure S3A* to *C*). Together, our results indicated that PIK-75 exerts potent growth inhibitory effects via the induction of apoptosis preferentially in *TAL1*-positive, AKT-activated T-ALL cells.

Sensitivity to PIK-75 is associated with the dependency on specific PI3K subunits

However, there were some exceptions of cell lines. SUP-T1 was TAL1-negative but sensitive to PIK-75, while PF-382 was TAL1-positive but relatively less sensitive. Thus, we made use of the DepMap database[29-32] to further examine the dependency of T-ALL cell lines on the PI3K-AKT pathway based on the CRISPR- or shRNA-mediated genetic inhibition (*Online Supplementary Table S5*).

This analysis demonstrated that Jurkat (TAL1-positive, PIK-75-sensitive cell line) was indeed highly dependent on p110γ/PIK3CG, one of PI3K subunits, as shown by negative score (growth inhibition) after CRISPR-based growth inhibition. In contrast, DND-41 (insensitive line) was not dependent on any of PI3K subunits. Notably, SUP-T1 cells (TAL1-negative, sensitive line) was strongly dependent on p110α/PIK3CA, as supported by both CRISPR and shRNA data. Additionally, we found that PF-382 (TAL1-positive, less sensitive) was dependent on p110δ/PIK3CD, while PIK-75 primarily targets p110α/PIK3CA and p110γ/PIK3CG but not p110δ/PIK3CD. Thus, PF-382 is less sensitive to PIK-75 likely due to the substate specificity of this drug. Together, these analyses indicated that the dependency on PI3K-AKT pathway is one of main determinants associated with drug sensitivity.

PIK-75 inhibits the phosphorylation of AKT and RNA polymerase II

We next investigated the molecular mechanism of growth inhibition by PIK-75. For this experiment, we used higher concentration (1 μM) to analyze the effect for both sensitive and insensitive lines under the same concentration. Indeed, PIK-75 treatment inhibited the phosphorylation of AKT in both sensitive and insensitive cell line (LOUCY) (Figure 4A). This suggested that insensitive cell lines may have another mechanism that can support their cell survival after PI3K inhibition.

As mentioned above, besides PI3K, PIK-75 has been known to inhibit other kinases including CDK (CDK7 and CDK9) and DNA-PK.[25,26] In fact, a decrease in the phosphorylation of

A

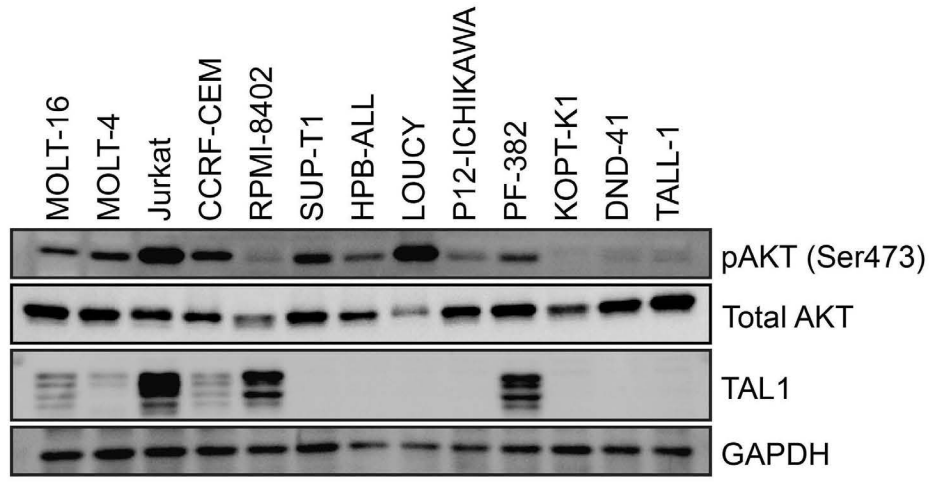

B

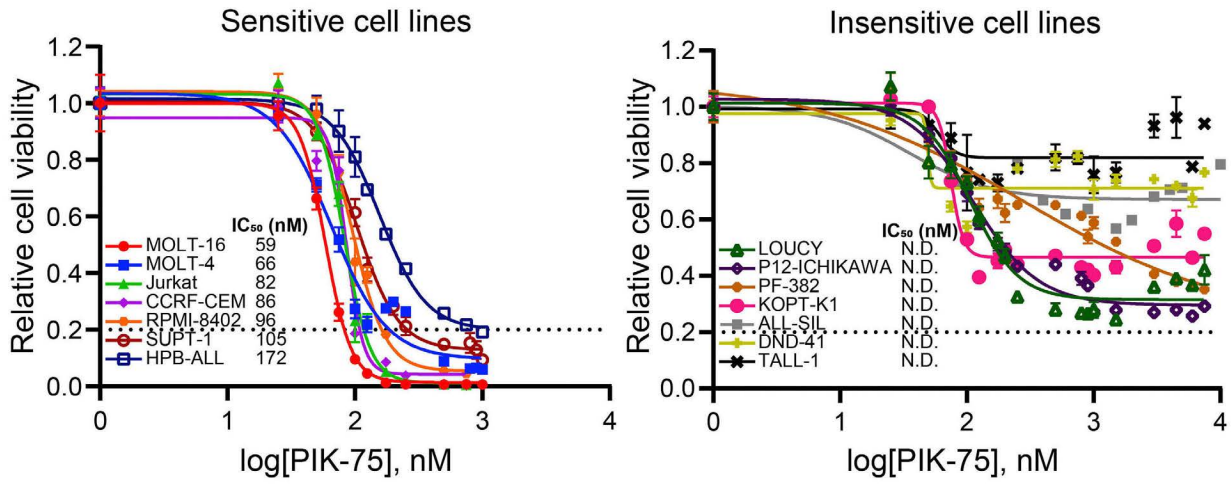

C

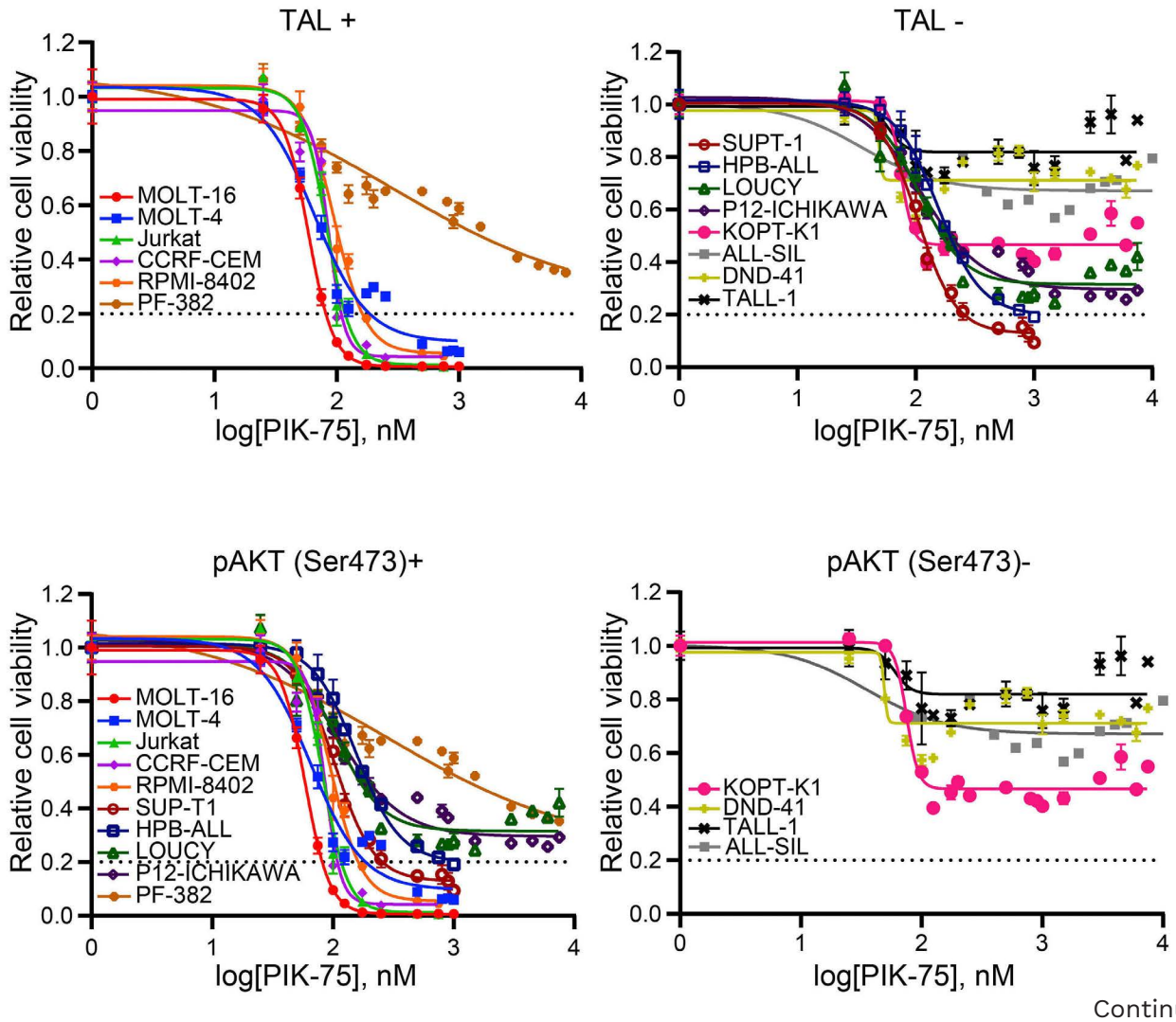

Continued on following page.

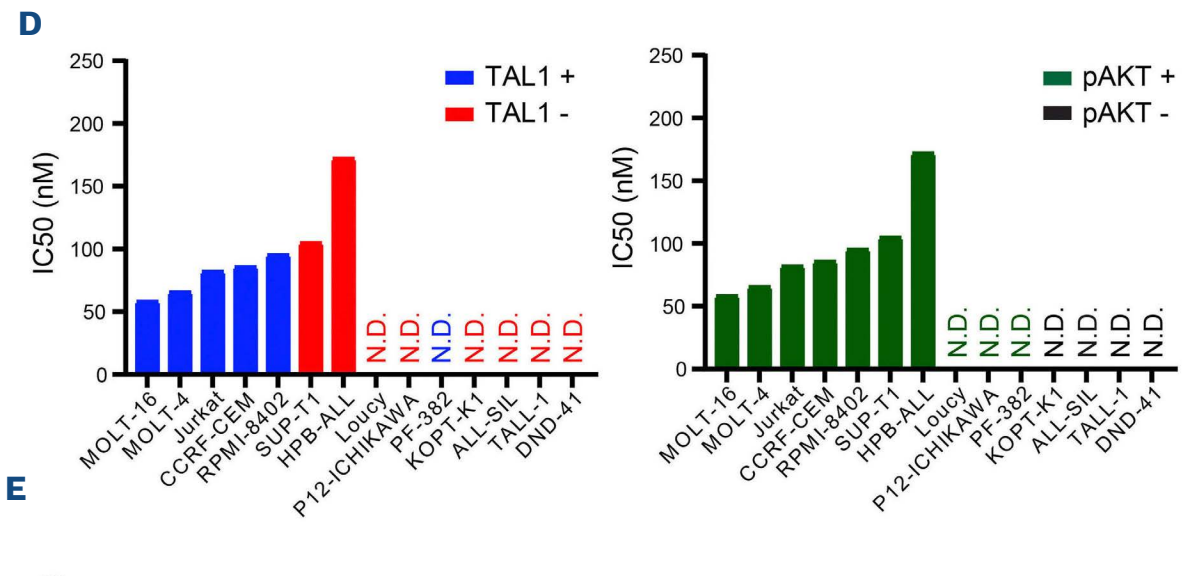

Figure 3. Growth inhibitory effect of PIK-75 on T-cell acute lymphoblastic leukemia cell lines. (A) Western blot showing the expression of phosphorylated AKT and TAL1 in T-cell acute lymphoblastic leukemia (T-ALL) cell lines. (B and C) T-ALL cell lines were treated with PIK-75. Cell viability was measured after 24 hours by CellTiter-Glo. The values shown are the mean ± standard deviation of technical triplicates and are normalized to untreated cells. Cell lines with viability greater than 20% after treatment with 1 μM PIK-75 were considered to be insensitive. Not able to be determined (N.D.), half maximal inhibitory concentration (IC_{50}) values could not be determined by the dose response inhibition function using variable slope by GraphPad Prism. Cell lines grouped based on sensitivity to PIK-75 (B) or TAL1 and AKT status (C). (D) Cell lines ranked according to IC_{50} value. TAL1 and AKT status are annotated by color. (E) Jurkat cells were seeded at 10,000 cells per well, treated with dimethyl sulfoxide (DMSO) or PIK-75 (120 nM) for 4 hours and stained with Annexin V-APC and PI. The values shown are the proportions of the total population ± standard deviation of technical triplicates. Representative results from multiple independent experiments were shown (B to E).

RNA polymerase II at Ser 2 and 5 residues was observed in all treated cell lines, regardless of drug sensitivity (Figure 4A). We observed a significant increase in γH2AX, a surrogate marker of the DNA damage response mediated by DNA-PK,[33] in sensitive cell lines. In contrast, in insensitive cell lines, there was little to no increase in γH2AX (Figure 4B). Thus, our results indicated that PIK-75 mainly inhibits the activity of RNA polymerase II and AKT.

PIK-75 affects global transcription in T-cell acute lymphoblastic leukemia cells

Because PIK-75 inhibits the activation of RNA polymerase II via the inhibition of CDK, we next examined if it globally inhibits transcription or affects specific genes. We first analyzed the effect of PIK-75 on TAL1 targets at the mRNA level. qRT-PCR analysis demonstrated that the mRNA expression of multiple *GIMAP* genes was significantly downregulated after 4 hours of treatment in Jurkat (Figure 5A) and other cell lines (*Online Supplementary Figure 4A*). Similarly, the mRNA expression of other known targets of TAL1,[9,12,34] including *ARID5B*, *NKX3-1* and *MYB*, was also downregulated after treatment (Figure 5B). This trend was found from low doses of PIK-75 in a dose-dependent manner (*Online Supplementary Figure S4B*).

In order to comprehensively analyze gene expression changes, we performed RNA-seq analysis of one representative sensitive cell line (Jurkat) and one insensitive cell line (DND-41) treated with DMSO (control) or PIK-75 for 4 hours at the IC_{80} of Jurkat. In order to analyze the global effect on transcription, we added synthesized RNA (ERCC spike-in) to the samples based on the cell number and normalized the expression values with or without the spike-in. Notably, when we analyzed the samples without the spike-in control, a large number of genes were significantly downregulated or upregulated after drug treatment in both cell lines (Figure 5C, top panels). Under this condition, spike-in RNA (shown in orange or purple) were overrepresented in the PIK-75-treated samples in both cell lines compared with the controls, indicating that the expression level of endogenous RNA were inappropriately represented. This suggested that the total pool of endogenous RNA might be reduced by PIK-75 treatment in both cell lines regardless of sensitivity. In fact, when we normalized expression values using spike-in, the number of differentially-expressed genes was largely diminished (Figure 5C, bottom panels). Importantly, there were still many differentially-expressed genes in the sensitive line (Jurkat), while there were very few changes observed in the insensitive line (DND-41) (Figure 5C; *Online Supplementary Table S6*). This result indicated that PIK-75 can globally affect RNA transcription in both cell lines, while it still affects specific molecular pathways in a sensitive cell line.

PIK-75 inhibits the expression of downstream targets of TAL1 in T-cell acute lymphoblastic leukemia cells

We then analyzed molecular pathways that were sensitive

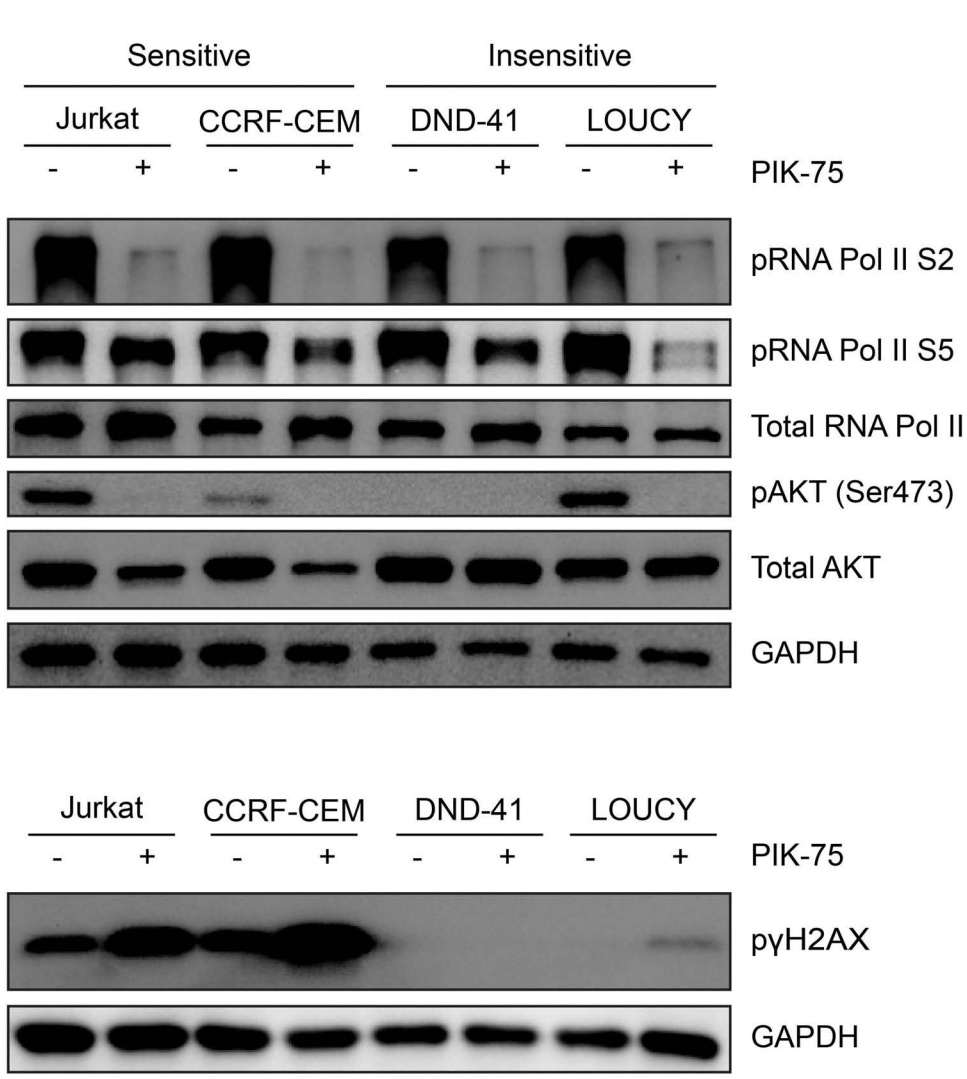

Figure 4. The effect of PIK-75 on target proteins and pathways. (A) Western blot showing the expression of phosphorylated AKT and RNA polymerase II in 4 T-cell acute lymphoblastic leukemia (T-ALL) cell lines (Jurkat, CCRF-CEM, DND-41, and LOUCY). All cell lines were treated with dimethyl sulfoxide (DMSO) or PIK-75 (1 μM). (B) Western blot analysis showing the expression of γH2AX in Jurkat, CCRF-CEM, DND-41, and LOUCY cells treated with either DMSO or PIK-75 (1 μM).

to PIK-75 treatment in a sensitive cell line. Consistent with the qRT-PCR results, GSEA showed that many of high-confidence targets of TAL1 were significantly downregulated by PIK-75 treatment (Figure 6A). In addition, genes that are associated with super-enhancers in Jurkat cells but not in normal thymus were also significantly downregulated. Heatmap analysis also demonstrated the downregulation of TAL1 target genes after PIK-75 treatment in Jurkat cells (Figure 6B). This suggested that although PIK-75 globally affects gene expression, it preferentially inhibits key oncogenic pathways, as previously reported for CDK7 inhibitors (THZ1) or BRD4 inhibitors (JQ1).[24,35,36] Similarly, GO analysis with Enrichr indicated that many downregulated genes were involved in transcription pathways (Figure 6C).

Related to this point, we also compared the growth inhibitory effect of PIK-75 with THZ1, JQ1 and DBZ (GSI) *(Online Supplementary Figure S5A*). This result indicated two cell lines (Jurkat and HPB-ALL) which were sensitive to PIK-75 were also sensitive to THZ1, while two cell lines (DND-41 and TALL-1) which were insensitive to PIK-75 were also relatively insensitive to THZ1. In contrast, no strong cytotoxicity or consistent trend were observed for JQ1 in our setting. As expected, both THZ1 and JQ1 inhibited the expression of *GIMAPs* and *ARID5B* (*Online Supplementary Figure S5B*) which are regulated under super-enhancers.[12,13]

Of note, expression of known downstream targets of NOTCH1, such as *HES1* and *MYC*, were downregulated by DBZ but not by PIK-75 in Jurkat cells (*Online Supplementary Figure S5C*). This result suggested that PIK-75's effect is independent from NOTCH1 activity.

Activation of the JAK-STAT pathway confers drug resistance to PIK-75 treatment

Notably, we found that in the insensitive cell line (DND-41), the *CISH* and *PIM1* genes were significantly upregulated after treatment (Figure 7A; *Online Supplementary Table S6*). These genes have been known to serve downstream of the JAK-STAT pathway, which is primarily activated by IL-7 receptor (IL-7R) signaling.[37,38] In fact, phosphorylation of STAT5 protein was observed in two insensitive lines (KOPT-K1 and DND-41) at the basal level (Figure 7B). Phosphorylation of multiple JAK and STAT proteins increased after treatment with PIK-75 in DND-41 cells but not in Jurkat cells (Figure 7C). Hence, we postulated that activation of the JAK-STAT pathway may be related to the sensitivity to PIK-75.

In order to further confirm this finding, we tested PIK-75 under two other conditions: i) in HPB-ALL cells, which exhibit the constitutive phosphorylation of AKT (Figure 3A) and also express IL-7R that can activate JAK-STAT pathway after IL-7 treatment, and ii) in SUP-T1 cells, which cannot activate this pathway after IL-7 treatment. We first pretreated HPB-ALL cells with IL-7 ligand to induce JAK-STAT activation (Figure 7D) and then treated them with PIK-75. Of note, this cell line is sensitive to PIK-75 in the absence of IL-7 (Figures 3B and 7E), thus

suggesting that it is dependent on AKT pathway. Remarkably, IL-7-treated cells were completely insensitive to PIK-75 treatment (Figure 7E), similar to DND-41 cells. The expression of BCL2, an anti-apoptotic protein that has been known as a downstream target of JAK-STAT pathway, was upregulated after IL-7 treatment (Figure 7D and F). This indicated that the growth inhibitory effect of PIK-75 likely via AKT inhibition can be rescued by the activation of JAK-STAT pathway. In contrast, in SUP-T1 cells, IL-7 treatment did not induce STAT activation or confer resistance to PIK-75 *(Online Supplementary Figure S6A* and *B*). We also utilized the DepMap dataset, which demonstrated that DND-41 was

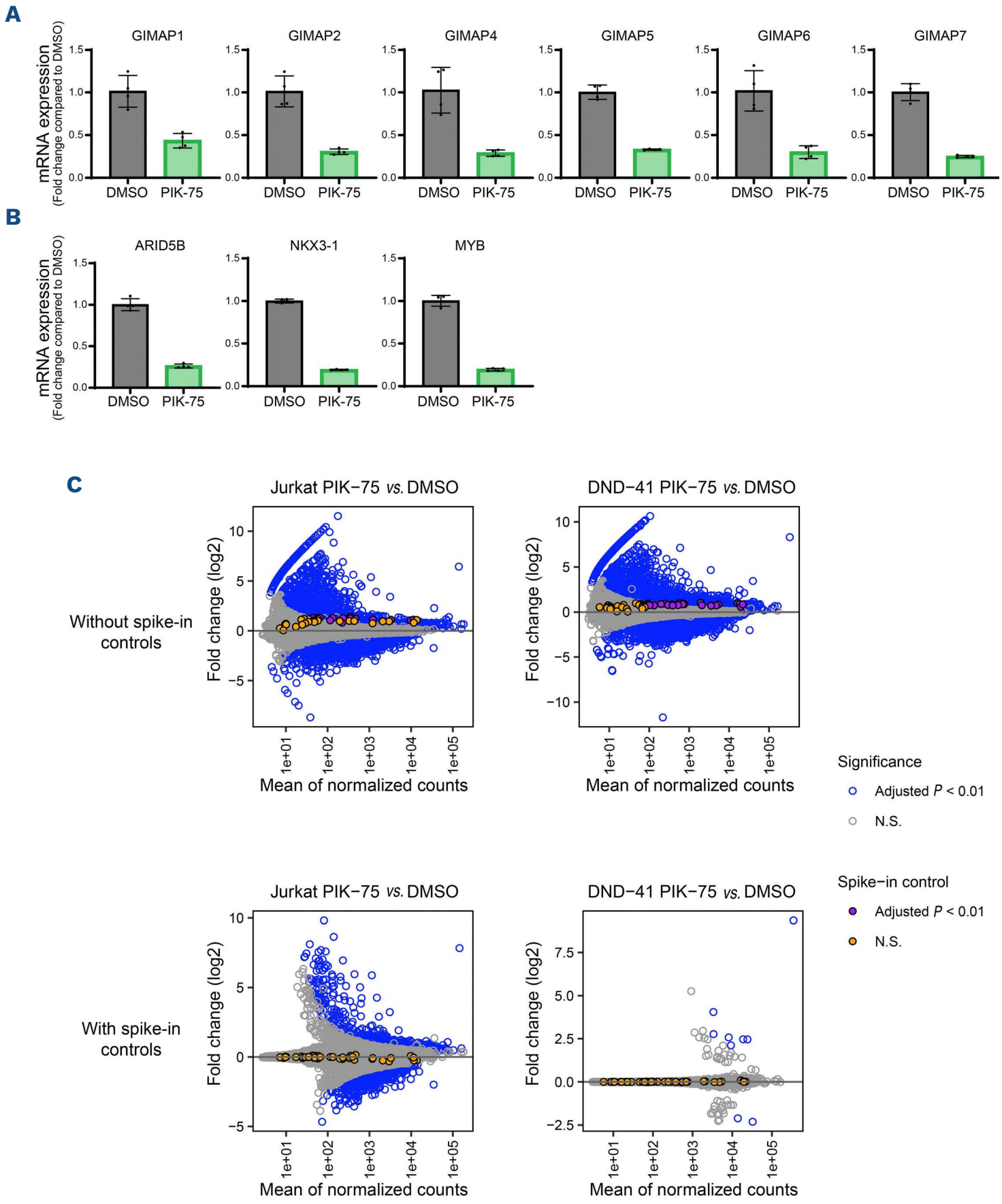

Figure 5. Gene expression changes after PIK-75 treatment in T-cell acute lymphoblastic leukemia cells. (A and B) mRNA expression levels of *GIMAP* cluster genes (A) and other TAL1 targets (B) in Jurkat cells 4 hours after PIK-75 treatment (120 nM). Expression values were normalized to spike-in RNA and shown as individual dots and mean ± standard deviation of biological duplicates and technical duplicates. Representative results from multiple independent experiments were shown. (C) MA plot showing the average of normalized counts *vs.* $\log_2$-normalized fold change (FC) between samples treated with dimethyl sulfoxide (DMSO) and PIK-75, estimated using DESeq2 with or without spike-in normalization. Each individual gene and spike-in control are represented by a single dot. RefSeq genes that showed statistically significant differences (adjusted *P* value <0.01) are colored blue. Similarly, spike-in controls are shown in purple (adjusted *P* value <0.01) or orange. N.S.: not significant.

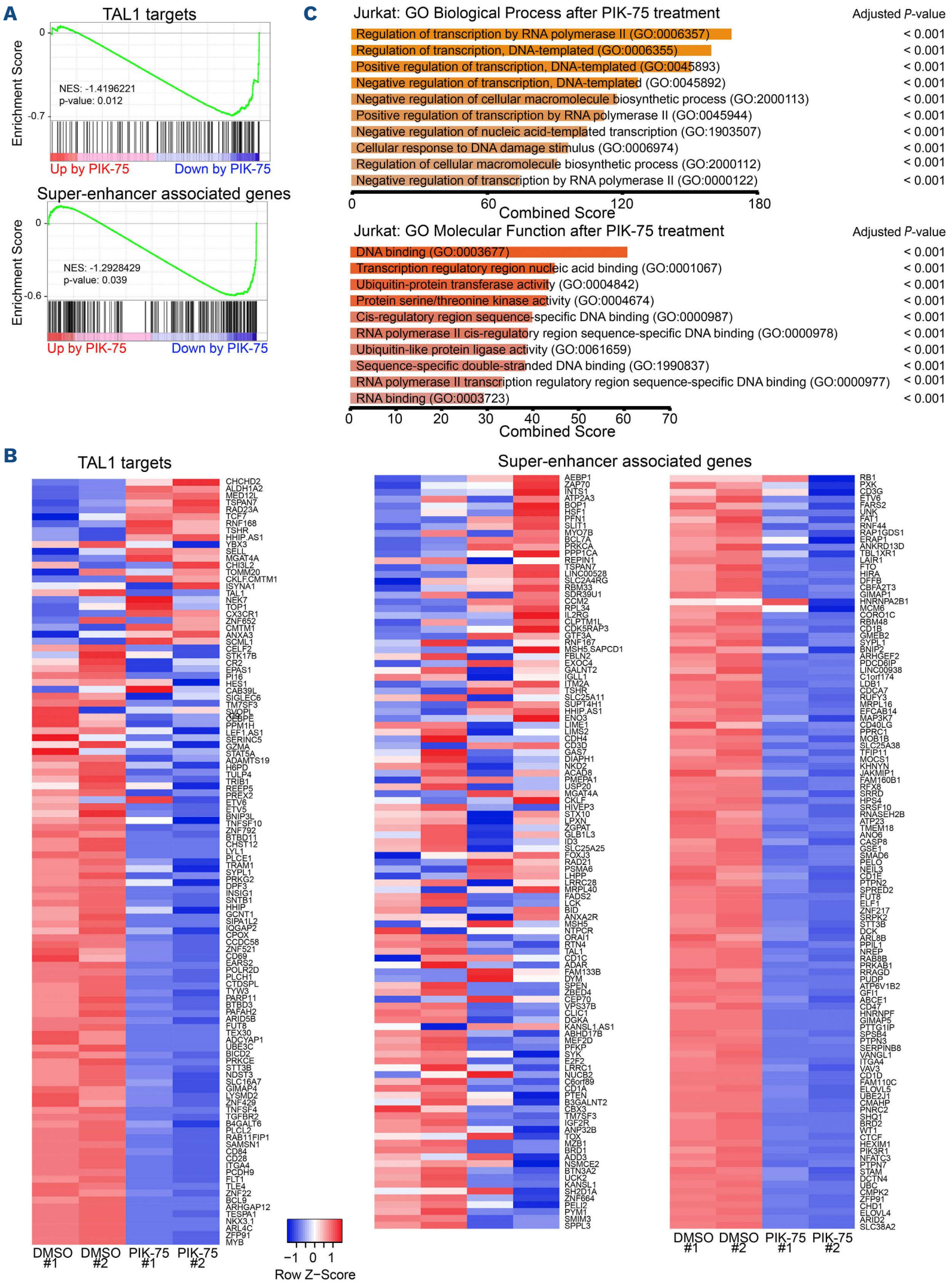

Figure 6. The effect of PIK-75 on TAL1 targets and super-enhancer-associated genes. (A) Gene set enrichment analysis (GSEA) to determine overall correlation between the change in gene expression after PIK-75 treatment in Jurkat cells and specific set of genes. The list of high-confidence TAL1 target genes (bound by TAL1 and downregulated after *TAL1* knockdown in Jurkat cells) and of super-enhancer associated genes were used as gene sets. (B) Heatmap showing the expression of TAL1 targets after PIK-75 treatment. (C) Gene ontology analysis was performed using genes that were significantly downregulated (base mean >10, $\log_2$ (fold change) × -$\log_{10}$ (*P* value) <-1, adjusted *P* value <0.01) in Jurkat cells 4 hours after PIK-75 treatment. The top 10 terms were selected according to the adjusted *P* value and are shown according to the combined score. Adjusted *P* value was calculated using Fisher's exact test.

strongly dependent on *IL-7R* and *JAK1* while SUP-T1 was not affected by *IL-7R* knockdown.

In order to further analyze the effect of JAK-STAT activation, we overexpressed BCL2 in Jurkat cells expressing the *GIMAP* reporter construct. In this setting, BCL2 expression was able to rescue growth inhibitory effect of PIK-75; however, luciferase activity was still inhibited (*Online Supplementary Figure S6C* and *D*). This result indicated that although BCL2 overexpression can sustain cell viability, it does not affect enhancer activity. Hence, mechanism of drug resistance by JAK-STAT signaling is likely due to the compensation of cell survival pathway but not due to the

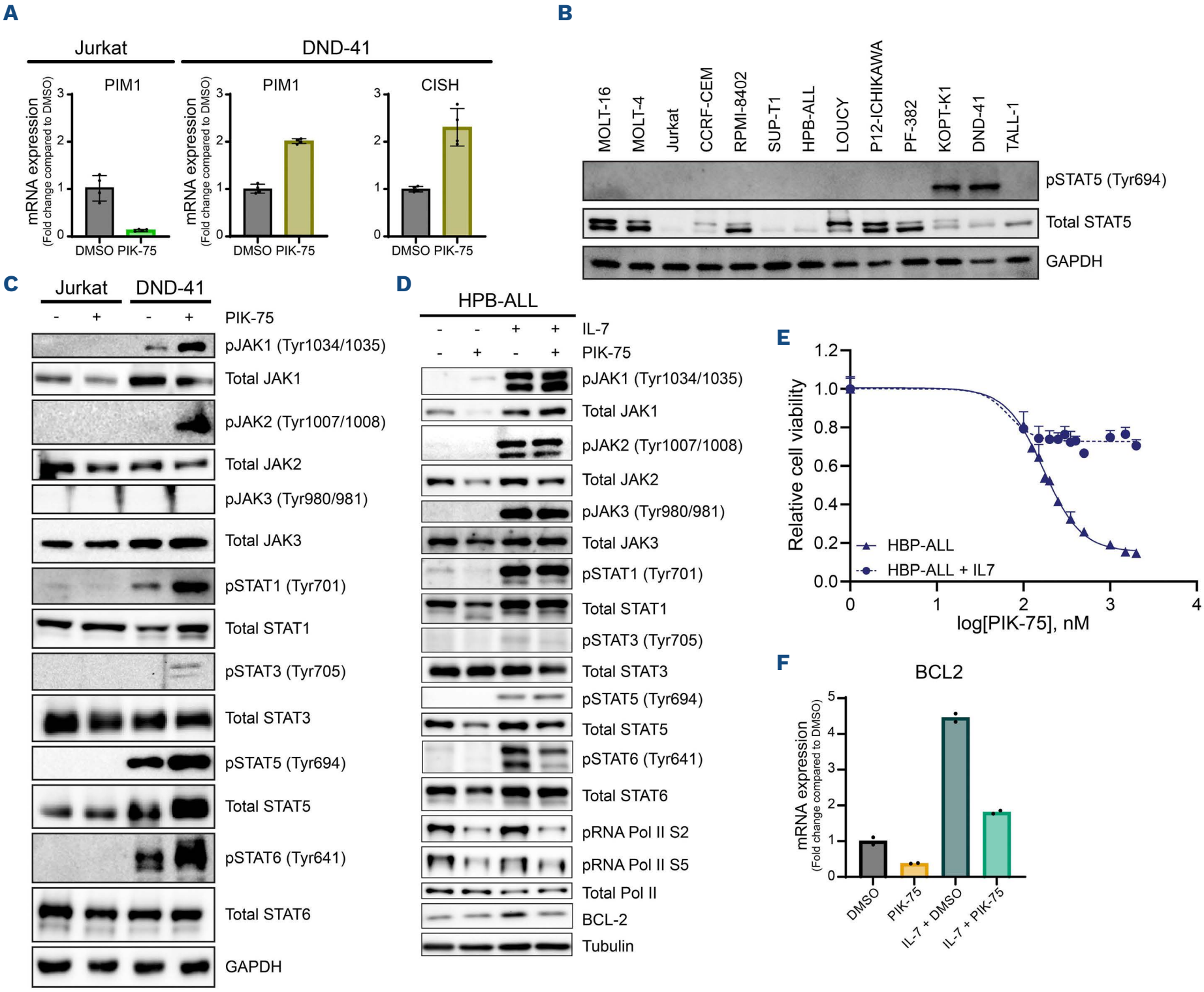

Figure 7. Potential involvement of JAK-STAT pathway in drug sensitivity to PIK-75. (A) mRNA expression levels of *PIM1* and *CISH* in Jurkat and DND-41 cells 4 hours after PIK-75 treatment (120 nM). Expression values were normalized to spike-in RNA and shown as individual dots and mean ± standard deviation of biological duplicates and technical duplicates. Representative results from multiple independent experiments were shown. (B) Western blot analysis showing the expression of phosphorylated STAT5 proteins in a panel of T-cell acute lymphoblastic leukemia (T-ALL) cell lines. (C) Western blot analysis showing the expression of multiple JAK and STAT proteins and their phosphorylated forms in Jurkat and DND-41 cell lines after treatment with dimethyl sulfoxide (DMSO) (control) or PIK-75 (120 nM) for 4 hours. (D) Western blot analysis showing the expression of phosphorylated JAK and STAT proteins as well as BCL2 protein with or without IL-7 induction and PIK-75 treatment (HPB-ALL half maximal inhibitory concentration [IC_{50}] =640 nM). (E) HPB-ALL was induced with IL-7 (50 ng/mL) for 24 hours before treatment with PIK-75. Cell viability was measured after 24 hours by CellTiter-Glo. The values shown are the mean ± standard deviation of technical triplicates and are normalized to untreated cells. (F) mRNA expression level of *BCL2* in HPB-ALL cells after 24 hours of IL-7 treatment and/or 4 hours of PIK-75 treatment (640 nM) was measured by qunatitative reverse transcription polymerase chain reaction (qRT-PCR). Expression values were normalized to spike-in RNA and shown as individual dots and mean of technical duplicates. Representative results from multiple independent experiments were shown.

interference of enhancer activity. Together, these findings indicated that JAK-STAT-active T-ALL cells are insensitive to PIK-75 treatment.

PIK-75 treatment inhibits the growth of primary T-cell acute lymphoblastic leukemia cells *ex vivo*

Finally, we investigated the potential therapeutic application of PIK-75. We analyzed the effect of PIK-75 on two human primary T-ALL cells (DFCI-9 and DFCI-15) propagated in a PDX model. Indeed, both DFCI-9 and DFCI-15 samples were sensitive to PIK-75, with IC_{50} values of 118 nM and 112 nM, respectively (Figure 8A). Similarly, we observed a reduction in phosphorylated RNA polymerase II and AKT after PIK-75 treatment in DFCI-15 cells (Figure 8B).

Discussion

In this study, we identified PIK-75 as one of top hit compounds from a chemical screening. This drug exerts potent antitumor effects *in vitro* via the inhibition of two core oncogenic machineries supporting the proliferation and survival of T-ALL cells: i) a transcriptional program driven by oncogenic transcription factors (type A abnormality) and ii) the PI3K-AKT pathway (type B abnormality). Our results support previous findings on the preferential relationship between type A and B genetic abnormalities and demonstrate the feasibility of a therapeutic strategy concurrently targeting these mechanisms.

In human T-ALL, genetic abnormalities in PI3K-AKT pathway components are more frequently observed in the *TAL1*-positive T-ALL subgroup.[15,39] Under experimental conditions, overexpression of TAL1 together with the activated form of AKT promotes T-ALL cell growth in mouse cells, which demonstrated a cooperative effect between these two abnormalities.[40,41] Similar cooperative effects have been reported for the TLX and JAK-STAT pathways.[42,43] These studies suggested an oncogenic collaboration between specific type A and type B abnormalities. In line with this notion, our study demonstrated that *TAL1*-positive, AKT-activated cell lines are sensitive to PIK-75, while activation of the JAK-STAT pathway confers resistance to this drug. This also suggested that the survival of T-ALL cells is dependent on one specific type B signaling pathway in each subgroup (i.e., PI3K-AKT in TAL1 subgroup, and JAK-STAT in TLX subgroup).

However, previous studies showed that small-molecule inhibitors of PI3K or AKT require relatively high concentrations to inhibit cell growth by a single treatment, even though they can inhibit AKT activation.[44-46] In this regard, PIK-75 exhibited strong cytotoxicity at low doses. This is likely attributed to concurrent inhibition of RNA polymerase II activity. An early study by Gray and Young's groups showed that THZ1 can induce a strong growth inhibitory effect by inhibiting the general transcription machinery.[24] Similarly, inhibition of BRD4 by JQ1 induces potent cytotoxicity.[47,48] Importantly, these studies reported that genes associated with super-enhancers are preferentially downregulated after treatment with these inhibitors. In fact, we observed that many TAL1 targets and super-enhancer-associated genes, including *GIMAP* and *ARID5B*, were significantly downregulated. Thus, although this drug affects global transcription and does not directly target TAL1 protein, it predominantly affects the transcriptional program driven by TAL1. Importantly, PIK-75 showed a potent cytotoxicity, demonstrating the advantage of dual inhibition of RNA polymerase II and PI3K-AKT pathway.

It is noteworthy that the sensitivity to this drug is not attributed to NOTCH1 status but rather is inversely associated with sensitivity to GSI. Resistance to GSI is a common problem which prevents the application of this type of drug for T-ALL.[49] Previously, Look's group reported that several T-ALL cell lines (DND-41, HPB-ALL, TALL-1 and

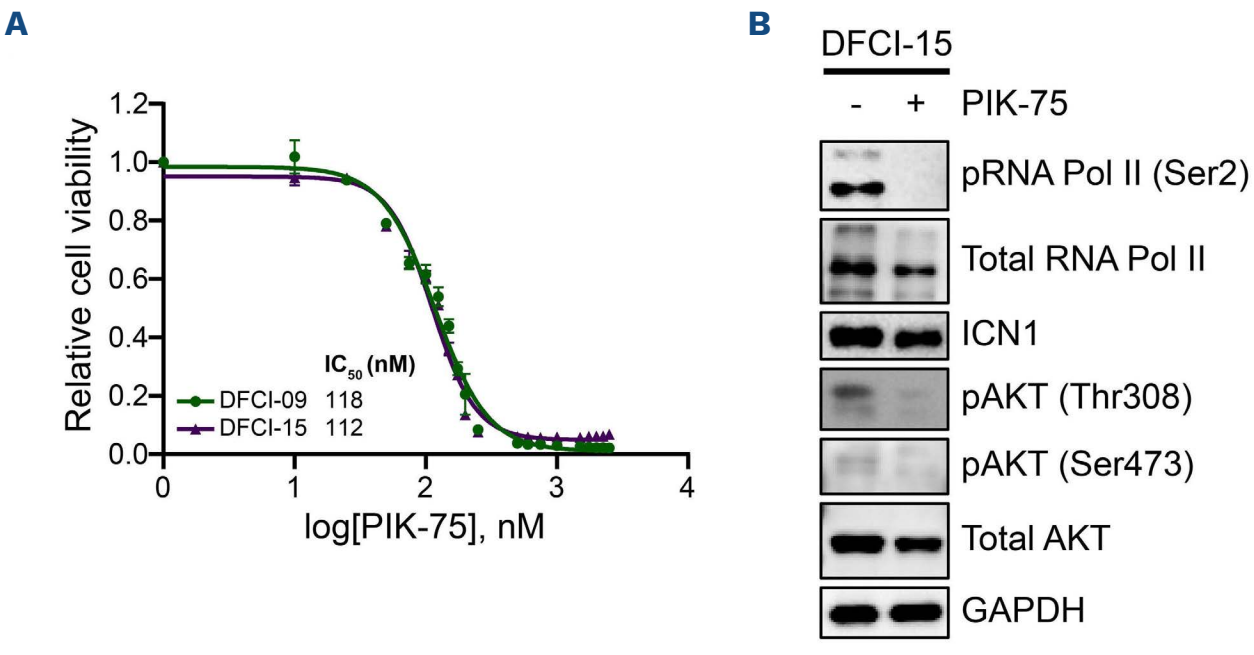

Figure 8. Growth inhibitory effect of PIK-75 on primary T-cell acute lymphoblastic leukemia cells. (A) Two patient-derived mouse xenograft samples (DFCI-9 and DFCI-15) were treated with PIK-75. Cell viability was measured after 24 hours by CellTiter-Glo. The values shown are the mean ± standard deviation of technical triplicates and are normalized to untreated cells. (B) Western blot analysis showing the expression of RNA polymerase II, AKT, and their phosphorylated forms in DFCI-15 cells after treatment with dimethyl sulfoxide (control) or PIK-75 (DFCI-15 half maximal inhibitory concentration [IC_{50}] =210 nM) for 4 hours.

KOPT-K1) are particularly sensitive to GSI, while many other cell lines are resistant.[27] Ferrando's group also reported that many GSI-resistant cell lines exhibit AKT activation, which confers drug resistance after GSI treatment.[44] These findings indicated that cell proliferation and survival in the GSI-resistant lines were supported by the PI3K-AKT pathway. In fact, GSI-resistant cell lines are relatively more sensitive than GSI-sensitive cell lines to PI3K/AKT inhibitors.[45] In line with this finding, we also demonstrated here that most GSI-resistant lines were sensitive to PIK-75, while four GSI-sensitive cell lines were insensitive. Together, our results highlight the exclusive relationship between oncogenic transcription factors (TAL1 *vs*. TLX), signaling pathways (PI3K-AKT *vs*. JAK-STAT) and drug sensitivity (PIK-75-sensitive *vs*. GSI-sensitive).

Taken together, our study demonstrated that PIK-75 concurrently inhibits two major oncogenic pathways (type A and B abnormalities), which is an ideal strategy to disrupt core machinery supporting the survival of T-ALL cells. Although PIK-75 is an old "forgotten" drug that might have been replaced with more specific PI3K-AKT inhibitors, it is worth revisiting the mechanism of this drug. Because PIK-75 was mainly studied before the concept of enhancer inhibition with CDK7 or BRD inhibitor was established,[24,36,37,47,48,50] its activity on CDK might be underestimated. Our study now demonstrates that multi-kinase specificity of PIK-75 rather provides an advantage for the treatment of T-ALL. However, we were also aware that one potential problem of this drug is the insolubility,[51] which prevents the application of PIK-75 *in vivo*. Thus, to move this drug forward to the clinical setting, further improvement of the chemical is necessary.

Disclosures

No conflicts of interest to disclose.

Contributions

FQL, ASYC, XZH, and MST performed the experiments; RY conducted the bioinformatic analyses. AEJY, SHT and TS supervised the study. FLQ and TS wrote the manuscript.

Funding

The research is supported by the National Medical Research Council of the Singapore Ministry of Health (NMRC/CIRG/1443/2016 to TS); by the National Research Foundation (NRF) Singapore and the Singapore Ministry of Education (MOE) under its Research Centers of Excellence initiative; and by the National University Cancer Institute Singapore, Yong Siew Yoon Research Grant and NCIS and NUS Cancer Program Seed Funding.

Data-sharing statement

RNA-seq data has been deposited in the Gene Expression Omnibus database under accession numbers GSE181435.

References

1. Look AT. Oncogenic transcription factors in the human acute leukemias. Science. 1997;278(5340):1059-1064.
2. Armstrong SA, Look AT. Molecular genetics of acute lymphoblastic leukemia. J Clin Oncol. 2005;23(26):6306-6315.
3. Aifantis I, Raetz E, Buonamici S. Molecular pathogenesis of T-cell leukaemia and lymphoma. Nat Rev Immunol. 2008;8(5):380-390.
4. Van Vlierberghe P, Pieters R, Beverloo HB, Meijerink JP. Molecular-genetic insights in paediatric T-cell acute lymphoblastic leukaemia. Br J Haematol. 2008;143(2):153-168.
5. Belver L, Ferrando A. The genetics and mechanisms of T cell acute lymphoblastic leukaemia. Nat Rev Cancer. 2016;16(8):494-507.
6. Brown L, Cheng JT, Chen Q, et al. Site-specific recombination of the tal-1 gene is a common occurrence in human T cell leukemia. EMBO J. 1990;9(10):3343-3351.
7. Ferrando AA, Neuberg DS, Staunton J, et al. Gene expression signatures define novel oncogenic pathways in T cell acute lymphoblastic leukemia. Cancer Cell. 2002;1(1):75-87.
8. Gianni F, Belver L, Ferrando A. The genetics and mechanisms of T-cell acute lymphoblastic leukemia. Cold Spring Harb Perspect Med. 2020;10(3):a035246.
9. Sanda T, Lawton LN, Barrasa MI, et al. Core transcriptional regulatory circuit controlled by the TAL1 complex in human T cell acute lymphoblastic leukemia. Cancer Cell. 2012;22(2):209-221.
10. Tan TK, Zhang C, Sanda T. Oncogenic transcriptional program driven by TAL1 in T-cell acute lymphoblastic leukemia. Int J Hematol. 2019;109(1):5-17.
11. Tan SH, Yam AW, Lawton LN, et al. TRIB2 reinforces the oncogenic transcriptional program controlled by the TAL1 complex in T-cell acute lymphoblastic leukemia. Leukemia. 2016;30(4):959-962.
12. Leong WZ, Tan SH, Ngoc PCT, et al. ARID5B as a critical downstream target of the TAL1 complex that activates the oncogenic transcriptional program and promotes T-cell leukemogenesis. Genes Dev. 2017;31(23-24):2343-2360.
13. Liau WS, Tan SH, Ngoc PCT, et al. Aberrant activation of the GIMAP enhancer by oncogenic transcription factors in T-cell acute lymphoblastic leukemia. Leukemia. 2017;31(8):1798-1807.
14. Weng AP, Ferrando AA, Lee W, et al. Activating mutations of NOTCH1 in human T cell acute lymphoblastic leukemia. Science. 2004;306(5694):269-271.
15. Liu Y, Easton J, Shao Y, et al. The genomic landscape of pediatric and young adult T-lineage acute lymphoblastic leukemia. Nat Genet. 2017;49(8):1211-1218.
16. Gutierrez A, Sanda T, Grebliunaite R, et al. High frequency of PTEN, PI3K, and AKT abnormalities in T-cell acute lymphoblastic leukemia. Blood. 2009;114(3):647-650.
17. Patro R, Duggal G, Love MI, Irizarry RA, Kingsford C. Salmon provides fast and bias-aware quantification of transcript expression. Nat Methods. 2017;14(4):417-419.
18. Soneson C, Love MI, Robinson MD. Differential analyses for RNA-seq: transcript-level estimates improve gene-level inferences.

F1000Res. 2015;4:1521.
19. Risso D, Ngai J, Speed TP, Dudoit S. Normalization of RNA-seq data using factor analysis of control genes or samples. Nat Biotechnol. 2014;32(9):896-902.
20. Love MI, Huber W, Anders S. Moderated estimation of fold change and dispersion for RNA-seq data with DESeq2. Genome Biol. 2014;15(12):550.
21. Zhu A, Ibrahim JG, Love MI. Heavy-tailed prior distributions for sequence count data: removing the noise and preserving large differences. Bioinformatics. 2019;35(12):2084-2092.
22. Subramanian A, Tamayo P, Mootha VK, et al. Gene set enrichment analysis: a knowledge-based approach for interpreting genome-wide expression profiles. Proc Natl Acad Sci U S A. 2005;102(43):15545-15550.
23. Chen EY, Tan CM, Kou Y, et al. Enrichr: interactive and collaborative HTML5 gene list enrichment analysis tool. BMC Bioinformatics. 2013;14:128.
24. Kwiatkowski N, Zhang T, Rahl PB, et al. Targeting transcription regulation in cancer with a covalent CDK7 inhibitor. Nature. 2014;511(7511):616-620.
25. Knight ZA, Gonzalez B, Feldman ME, et al. A pharmacological map of the PI3-K family defines a role for p110alpha in insulin signaling. Cell. 2006;125(4):733-747.
26. Thomas D, Powell JA, Vergez F, et al. Targeting acute myeloid leukemia by dual inhibition of PI3K signaling and Cdk9-mediated Mcl-1 transcription. Blood. 2013;122(5):738-748.
27. O'Neil J, Grim J, Strack P, et al. FBW7 mutations in leukemic cells mediate NOTCH pathway activation and resistance to gamma-secretase inhibitors. J Exp Med. 2007;204(8):1813-1824.
28. De Keersmaecker K, Porcu M, Cox L, et al. NUP214-ABL1-mediated cell proliferation in T-cell acute lymphoblastic leukemia is dependent on the LCK kinase and various interacting proteins. Haematologica. 2014;99(1):85-93.
29. Dempster JM, Boyle I, Vazquez F, et al. Chronos: a cell population dynamics model of CRISPR experiments that improves inference of gene fitness effects. Genome Biol. 2021;22(1):343.
30. Meyers RM, Bryan JG, McFarland JM, et al. Computational correction of copy number effect improves specificity of CRISPR-Cas9 essentiality screens in cancer cells. Nat Genet. 2017;49(12):1779-1784.
31. Dempster J, Rossen J, Kazachkova M, et al. Extracting biological insights from the Project Achilles Genome-Scale CRISPR screens in cancer cell lines. bioRxiv. 2019. doi: https://doi.org/10.1101/720243 [preprint, not peer-reviewed].
32. Ghandi M, Huang FW, Jane-Valbuena J, et al. Next-generation characterization of the Cancer Cell Line Encyclopedia. Nature. 2019;569(7757):503-508.
33. An J, Huang YC, Xu QZ, et al. DNA-PKcs plays a dominant role in the regulation of H2AX phosphorylation in response to DNA damage and cell cycle progression. BMC Mol Biol. 2010;11:18.
34. Kusy S, Gerby B, Goardon N, et al. NKX3.1 is a direct TAL1 target gene that mediates proliferation of TAL1-expressing human T cell acute lymphoblastic leukemia. J Exp Med. 2010;207(10):2141-2156.
35. Chipumuro E, Marco E, Christensen CL, et al. CDK7 inhibition suppresses super-enhancer-linked oncogenic transcription in MYCN-driven cancer. Cell. 2014;159(5):1126-1139.
36. Loven J, Hoke HA, Lin CY, et al. Selective inhibition of tumor oncogenes by disruption of super-enhancers. Cell. 2013;153(2):320-334.
37. Ghazawi FM, Faller EM, Parmar P, El-Salfiti A, MacPherson PA. Suppressor of cytokine signaling (SOCS) proteins are induced by IL-7 and target surface CD127 protein for degradation in human CD8 T cells. Cell Immunol. 2016;306-307:41-52.
38. Narlik-Grassow M, Blanco-Aparicio C, Carnero A. The PIM family of serine/threonine kinases in cancer. Med Res Rev. 2014;34(1):136-159.
39. Kimura S, Seki M, Kawai T, et al. DNA methylation-based classification reveals difference between pediatric T-cell acute lymphoblastic leukemia and normal thymocytes. Leukemia. 2020;34(4):1163-1168.
40. Girardi T, Vicente C, Cools J, De Keersmaecker K. The genetics and molecular biology of T-ALL. Blood. 2017;129(9):1113-1123.
41. Bornschein S, Demeyer S, Stirparo R, et al. Defining the molecular basis of oncogenic cooperation between TAL1 expression and Pten deletion in T-ALL using a novel pro-T-cell model system. Leukemia. 2018;32(4):941-951.
42. Vicente C, Schwab C, Broux M, et al. Targeted sequencing identifies associations between IL7R-JAK mutations and epigenetic modulators in T-cell acute lymphoblastic leukemia. Haematologica. 2015;100(10):1301-1310.
43. Vanden Bempt M, Demeyer S, Broux M, et al. Cooperative enhancer activation by TLX1 and STAT5 drives development of NUP214-ABL1/TLX1-positive T cell acute lymphoblastic leukemia. Cancer Cell. 2018;34(2):271-285.e7.
44. Palomero T, Sulis ML, Cortina M, et al. Mutational loss of PTEN induces resistance to NOTCH1 inhibition in T-cell leukemia. Nat Med. 2007;13(10):1203-1210.
45. Sanda T, Li X, Gutierrez A, et al. Interconnecting molecular pathways in the pathogenesis and drug sensitivity of T-cell acute lymphoblastic leukemia. Blood. 2010;115(9):1735-1745.
46. Simioni C, Neri LM, Tabellini G, et al. Cytotoxic activity of the novel Akt inhibitor, MK-2206, in T-cell acute lymphoblastic leukemia. Leukemia. 2012;26(11):2336-2342.
47. King B, Trimarchi T, Reavie L, et al. The ubiquitin ligase FBXW7 modulates leukemia-initiating cell activity by regulating MYC stability. Cell. 2013;153(7):1552-1566.
48. Roderick JE, Tesell J, Shultz LD, et al. c-Myc inhibition prevents leukemia initiation in mice and impairs the growth of relapsed and induction failure pediatric T-ALL cells. Blood. 2014;123(7):1040-1050.
49. Real PJ, Ferrando AA. NOTCH inhibition and glucocorticoid therapy in T-cell acute lymphoblastic leukemia. Leukemia. 2009;23(8):1374-1377.
50. Vervoort SJ, Devlin JR, Kwiatkowski N, Teng M, Gray NS, Johnstone RW. Targeting transcription cycles in cancer. Nat Rev Cancer. 2022;22(1):5-24.
51. Talekar M, Ganta S, Amiji M, et al. Development of PIK-75 nanosuspension formulation with enhanced delivery efficiency and cytotoxicity for targeted anti-cancer therapy. Int J Pharm. 2013;450(1-2):278-289.